Chapter 3

Pulsar outer-magnetospheric accelerator (outer-gap) model

Pulsar lepton accelerator model contains many common features with the BH lepton acc. model.

Thus, let us review the pulsar case first
before investigating the BH-gap model.

§1 Quick review of γ-ray observations of pulsars

§2 Quick review of pulsar emission models

§1 Quick review of pulsar γ-ray observations

§1 γ-ray Pulsar Observations

Fermi/LAT has detected >200 pulsars above 100 MeV.

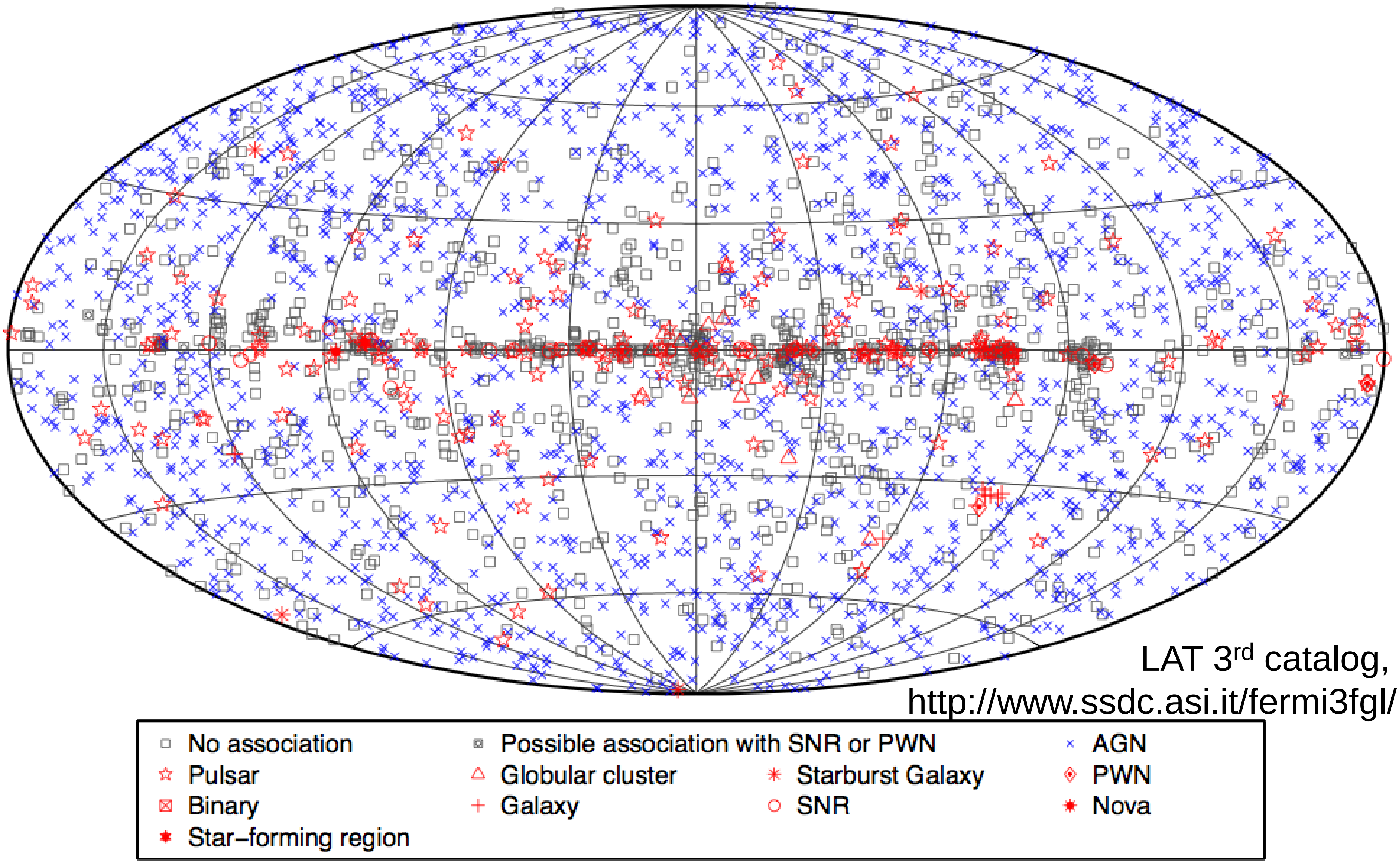

LAT 3rd catalog,
http://www.ssdc.asi.it/fermi3fgl/

§1 γ-ray Pulsar Observations

Recent IACTs found pulsed emission in 25GeV-2TeV from the Crab pulsar by VERITAS and MAGIC.

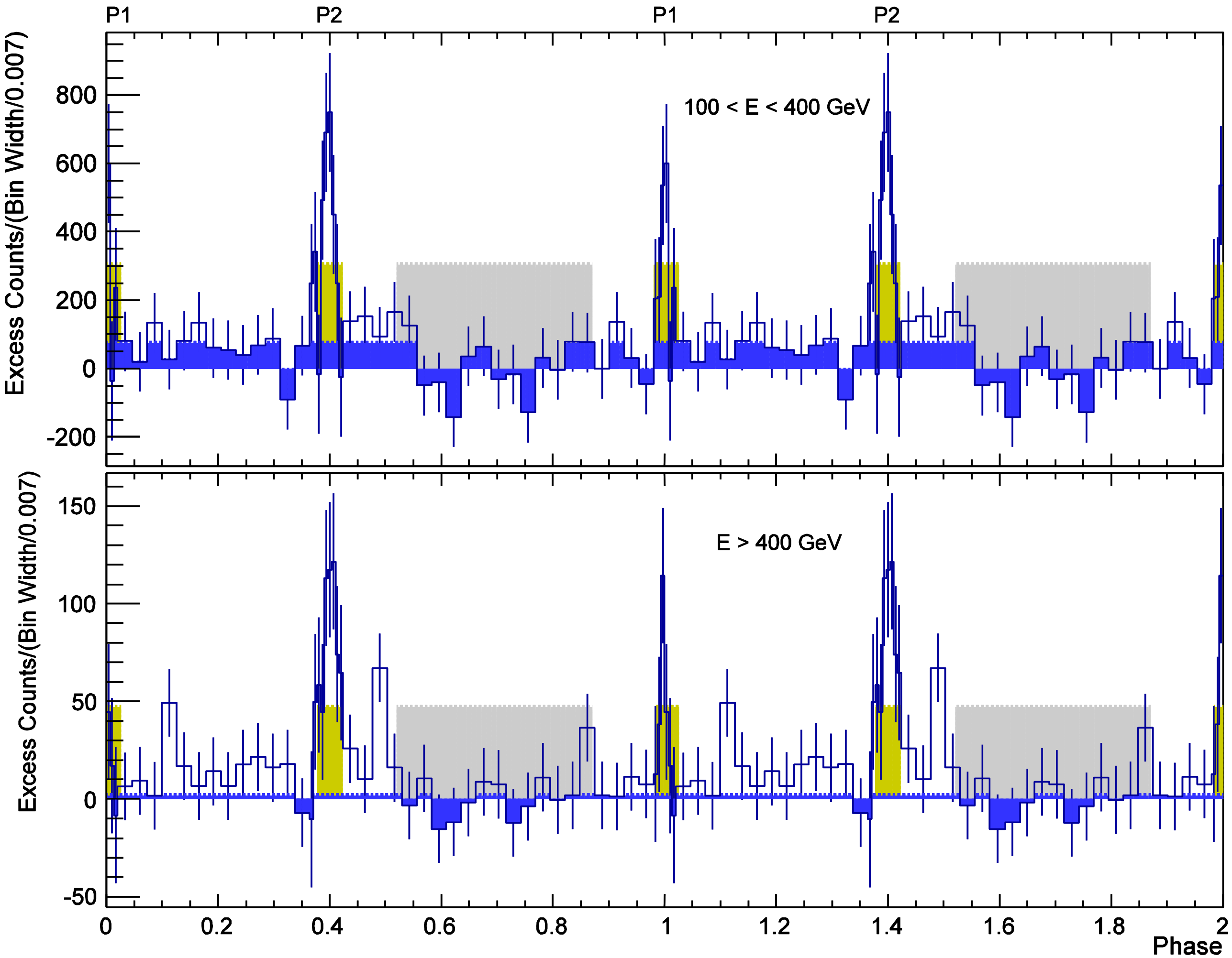

Light curve

MAGIC (100GeV-2TeV)

Ansoldi+ (2016, AA585,133)

§1 γ-ray Pulsar Observations

Recent IACTs found pulsed emission in 25GeV-2TeV from the Crab pulsar by VERITAS and MAGIC.

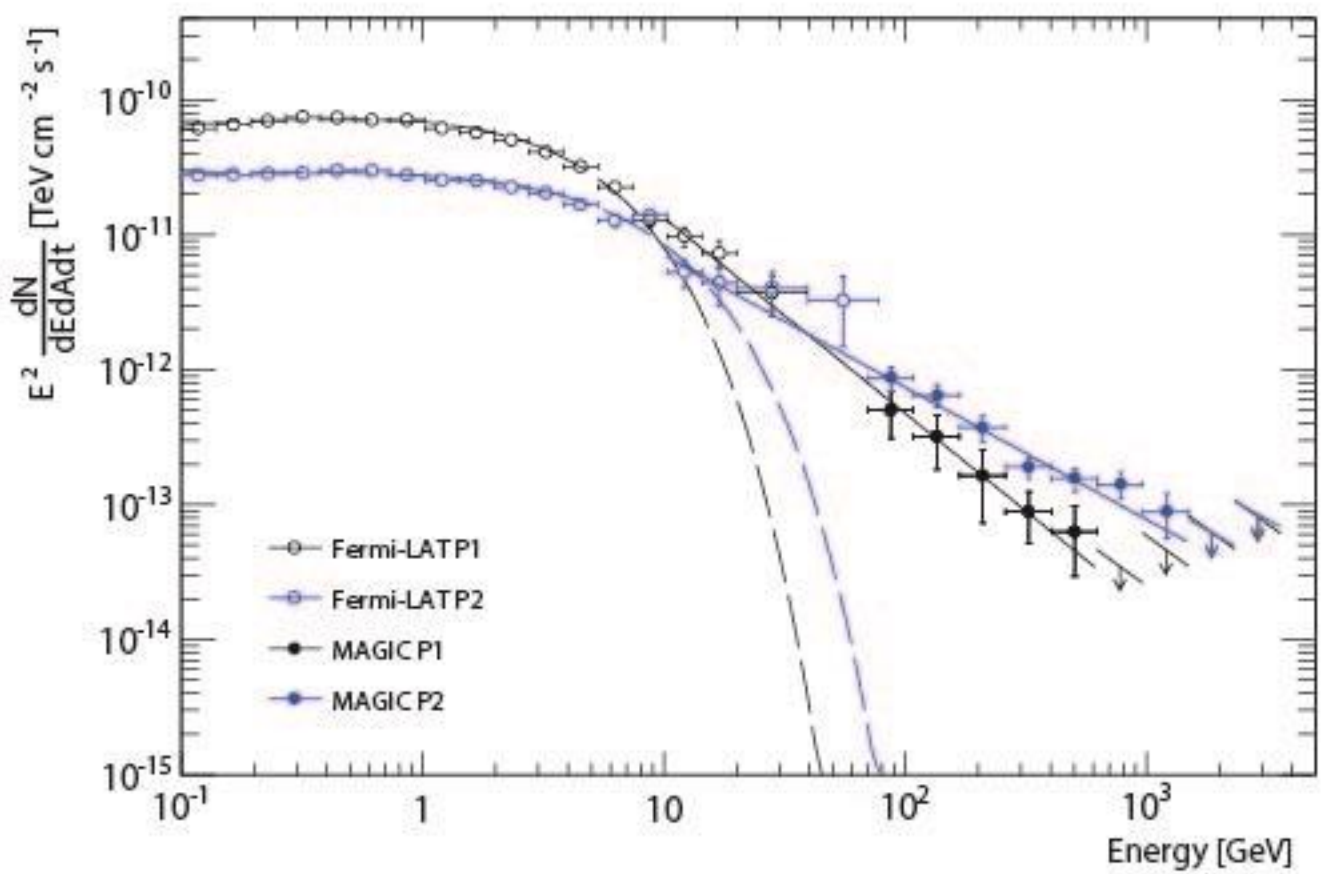

Pulsed spectrum

MAGIC (100GeV-2TeV)
Ansoldi+ (2016, AA585,133)

§1 γ-ray Pulsar Observations

VHE pulsation is also found from the Vela pulsar in 20-100 GeV.

H.E.S.S. (20-100 GeV) Abdalla + (2018, arXiv:1807.01202v2)

Light curve

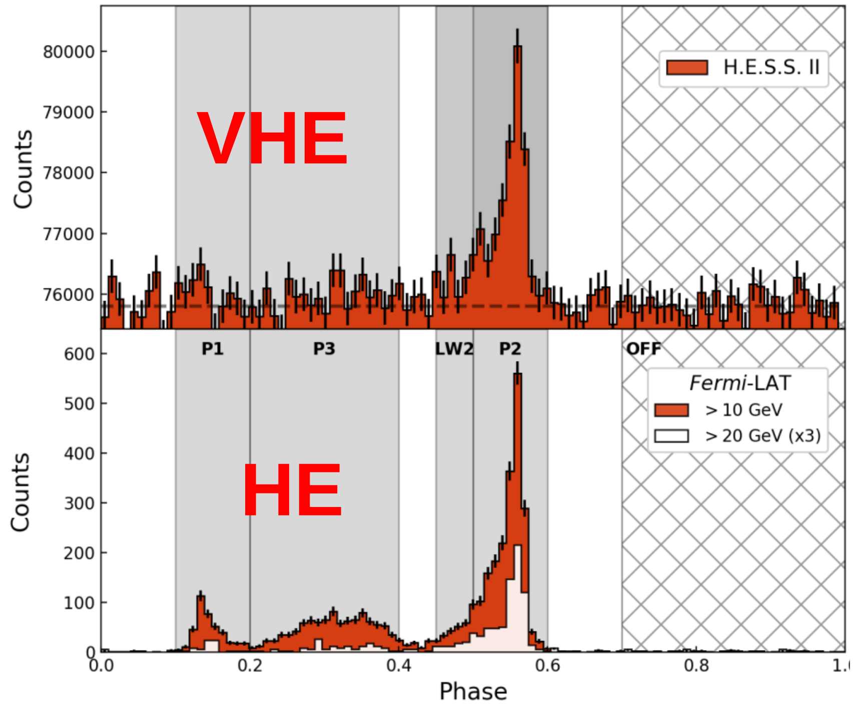

Pulsed pectrum

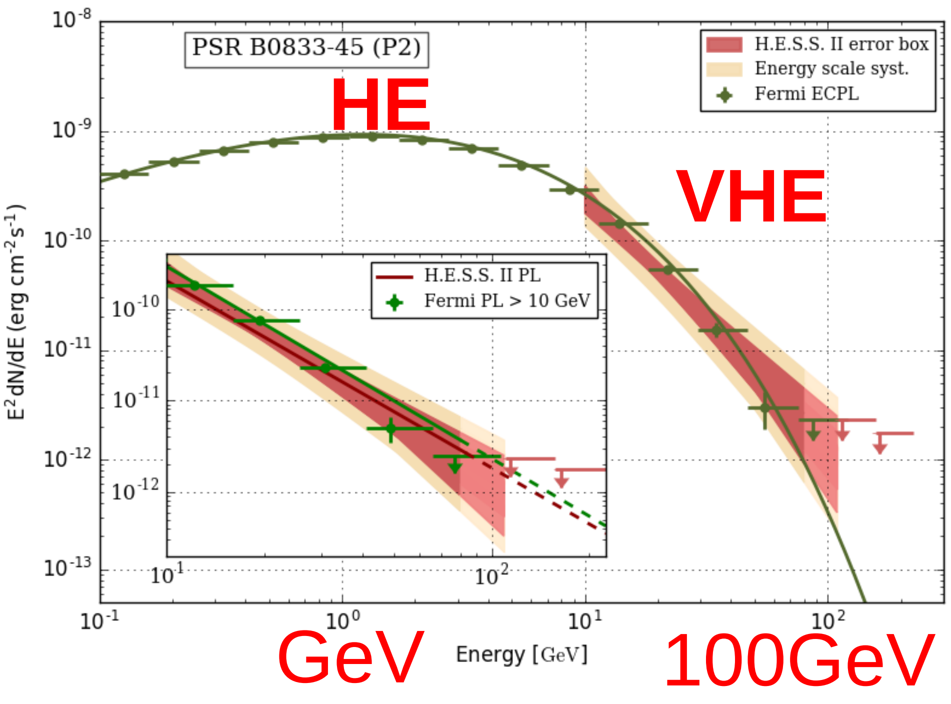

Broad-band spectra (pulsed)

- High-energy (> 100MeV) photons are emitted mainly via **curvature** process by ultra-relativistic (~10 TeV) $e^{\pm}$'s accelerated in pulsar magnetosphere.

- Above 20 GeV, **ICS by secondary/tertiary pairs** contributes.

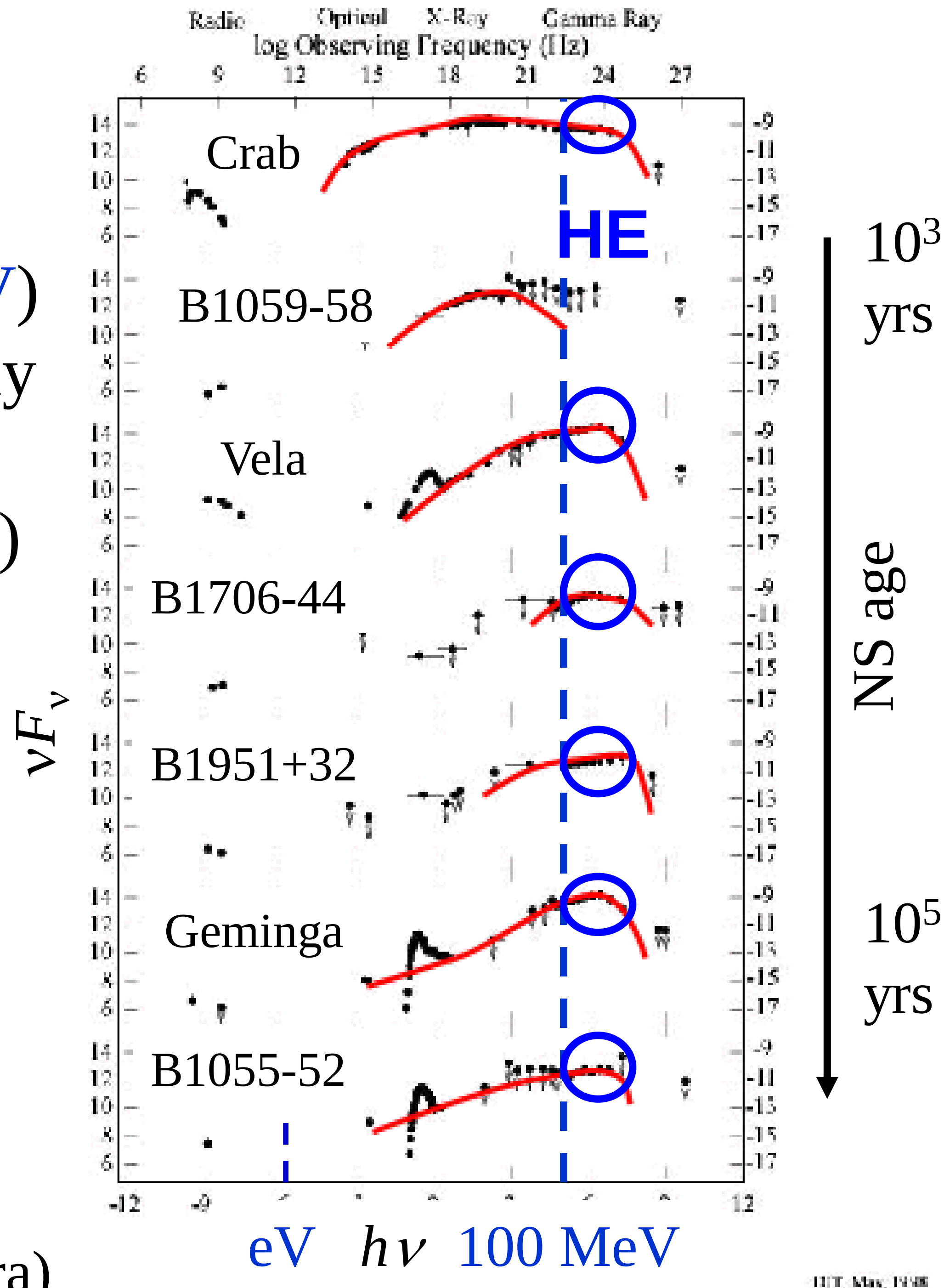

(Thompson, EGRET spectra)

Broad-band spectra (pulsed)

- High-energy (>100MeV) photons are emitted mainly via **curvature** process by ultra-relativistic (~10 TeV) $e^{\pm}$'s accelerated in pulsar magnetosphere.
- Above 20 GeV, **ICS by secondary/tertiary pairs** contributes.

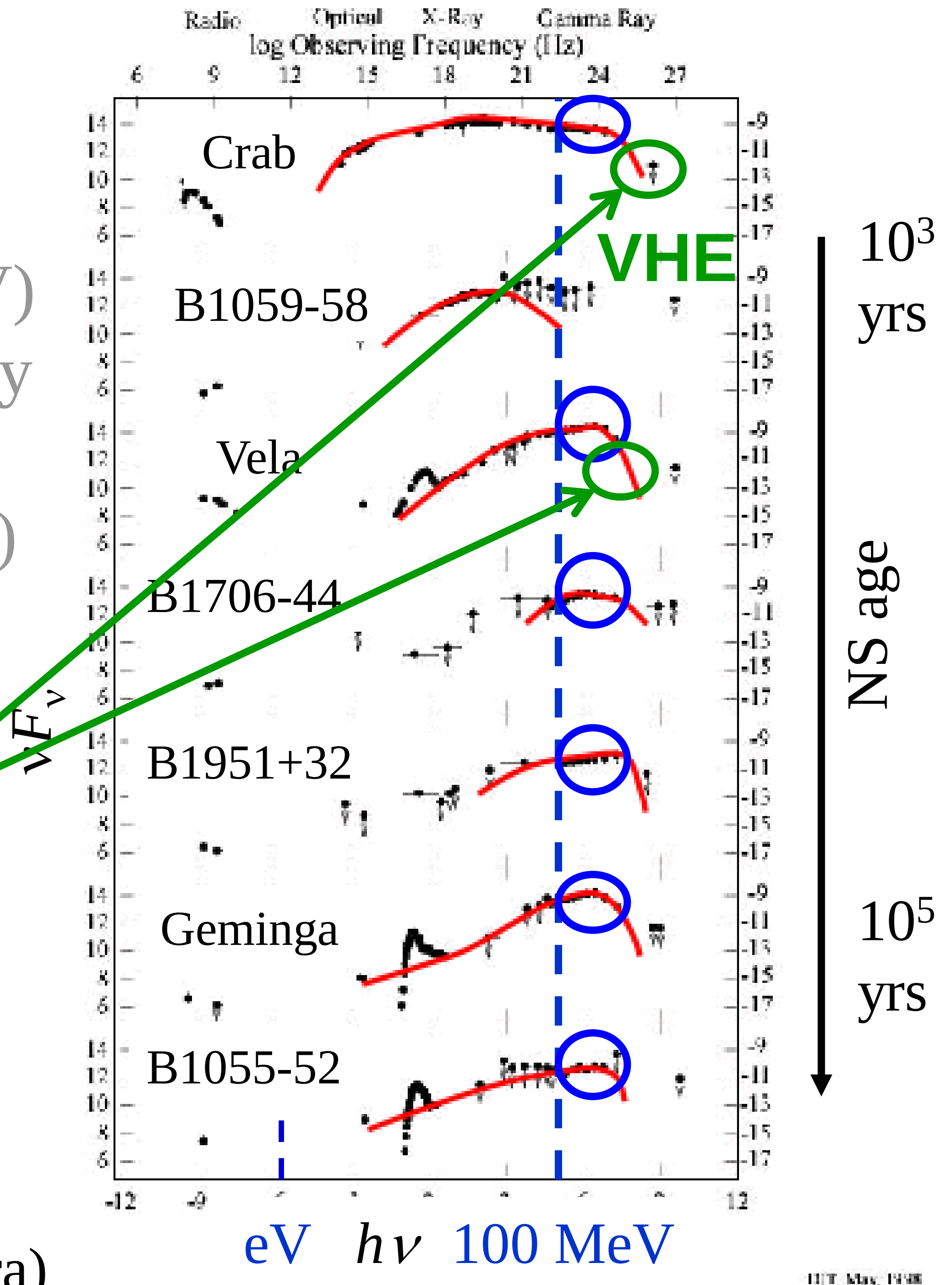

(Thompson, EGRET spectra)

§3 Quick Review of Representative Emission Models

Pulsars spin down as $\dot{E} = I\Omega\dot{\Omega}$.

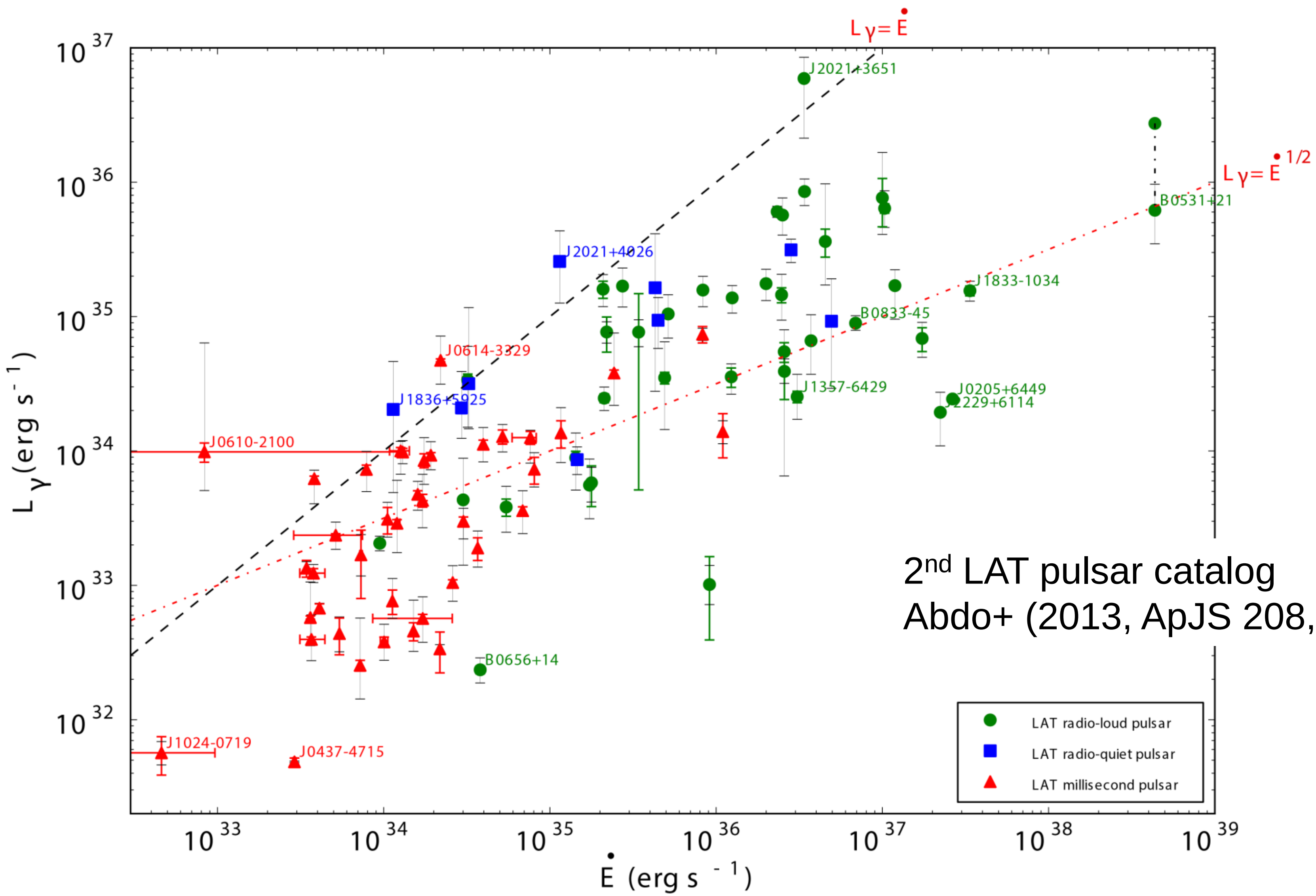

2nd LAT pulsar catalog
Abdo+ (2013, ApJS 208, 17)

§1 γ-ray Pulsar Observations

Next, let us consider how the NS's rotational energy is converted into the observed incoherent, HE/VHE emissions.

§2 Rotating Neutron Star Magnetosphere

§2 Rotating NS Magnetosphere

It is commonly accepted that pulsars are rapidly rotating, highly magnetized neutron stars.

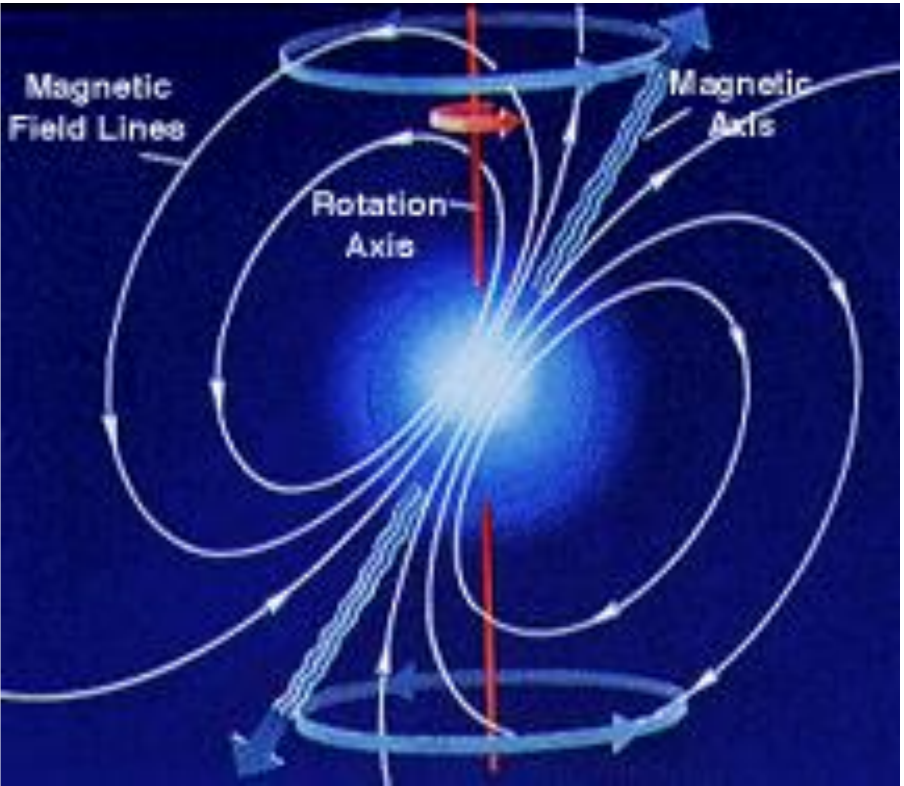

§2 Rotating NS Magnetosphere

The observed high-energy emissions are realized when the rotational energy of the NS is electro-dynamically extracted and partly dissipated in its magnetosphere.

(e.g., unipolar inductor)

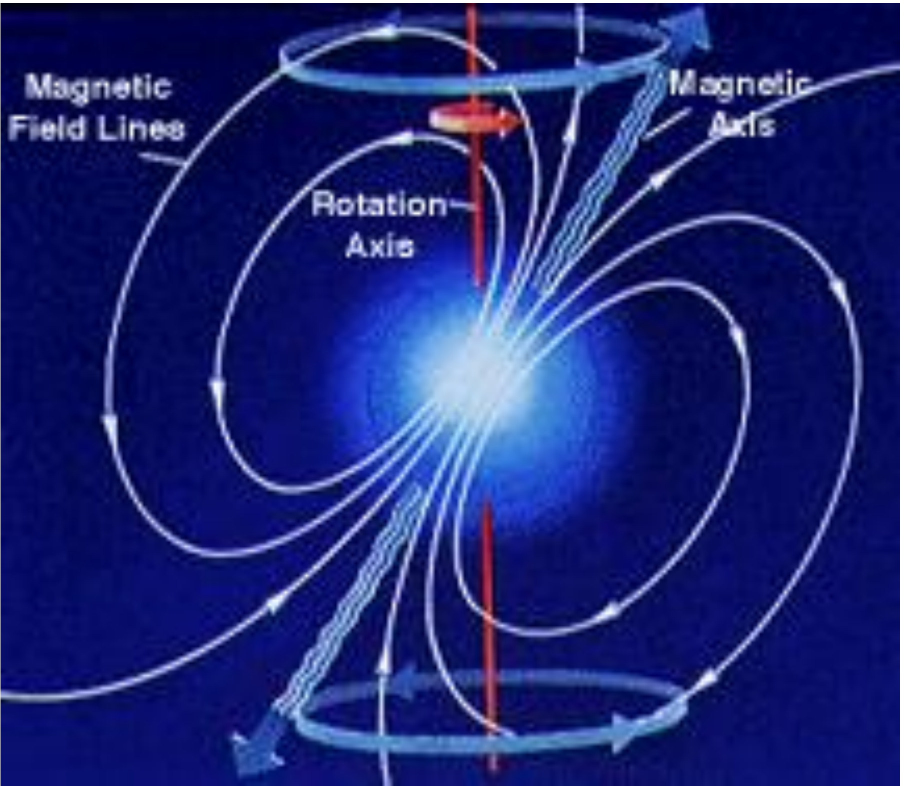

Fig.) Sketch of a pulsar. Magnetic and rotation axes are generally misaligned.

§2 Rotating NS Magnetosphere

Pulsar emissions result from electro-dynamical extraction of NS rotational energy.

(e.g., unipolar inductor)

On the spinning NS surface, EMF is exerted in the same way as a unipolar inductor (fig).

This EMF induces the global current, which extracts the rotational energy as Poynting flux.

In the case of pulsars, EMF is available only within the so-called 'open zone'.

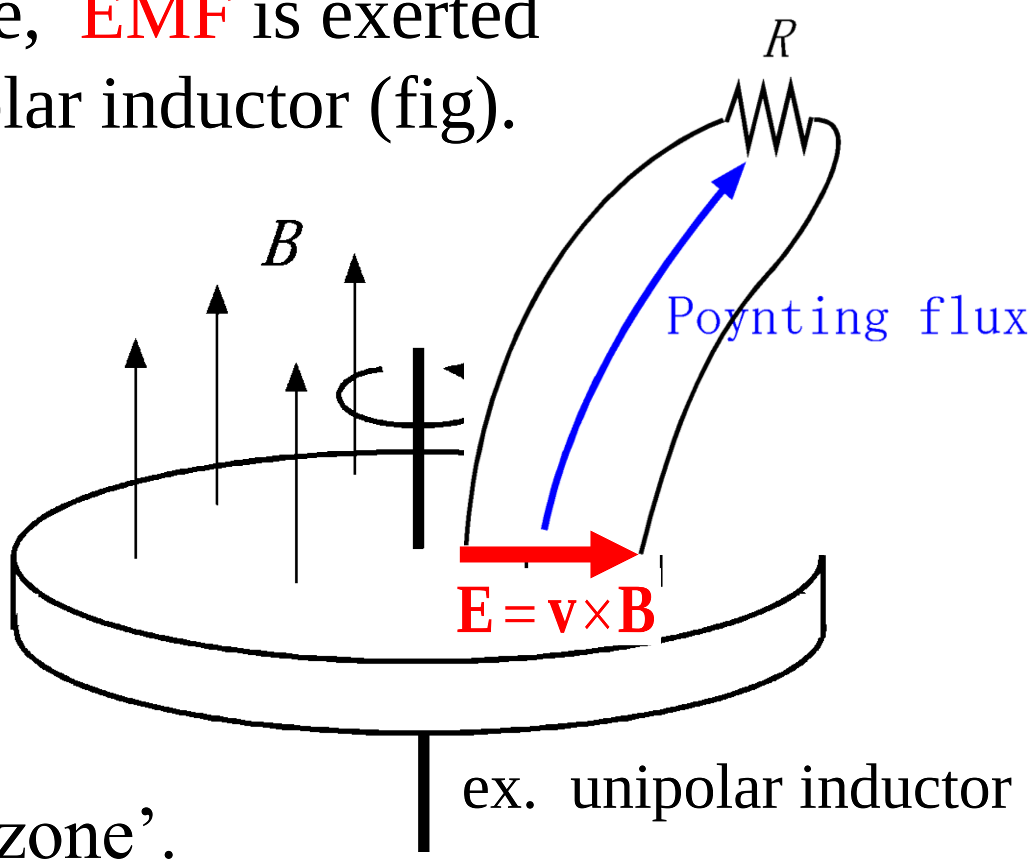

ex. unipolar inductor

§2 Rotating NS Magnetosphere

A rotating NS magnetosphere can be divided into open and closed zones.

Last-open field lines form the boundary of them.

In the open zone, $e^{\pm}$'s escape through the light cylinder as a pulsar wind.

In the closed zone, on the other hand, an $E_{\parallel}$ would be very quickly screened by the dense plasmas.

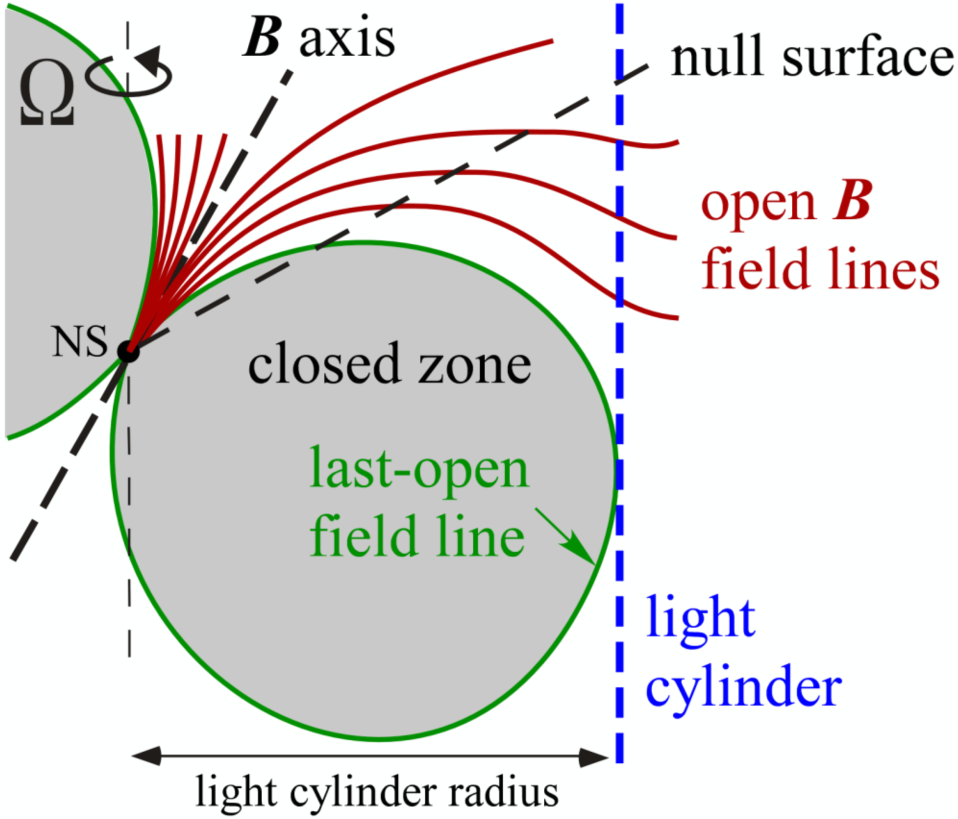

$\varpi_{LC} = 3\times10^8(\Omega/10^2\,\mathrm{rad\,s^{-1}})$ cm

§2 Rotating NS Magnetosphere

A rotating NS magnetosphere can be divided into open and closed zones.

Last-open field lines form the boundary of them.

In the open zone, $e^{\pm}$'s escape through the light cylinder as a pulsar wind.

In the closed zone, on the other hand, an $E_{\parallel}$ would be very quickly screened by the dense plasmas.

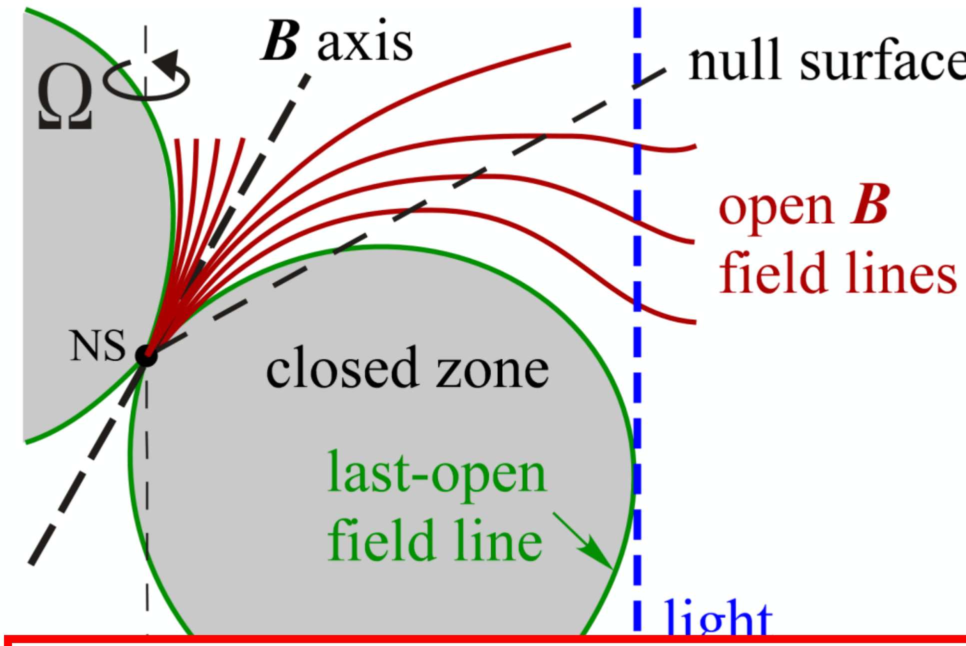

Thus, in all pulsar emission models, particle acceleration takes place only within the open zone.

§2 Rotating NS Magnetosphere

For typical high-energy pulsars, open zone occupies only a few degrees from ***B*** axis on the PC surface.

Available voltage in the open zone:

$$\mathrm{EMF} \sim \frac{\Omega^2 B_* r_*^3}{c^2} \sim 10^{15.5}\ \mathrm{V}$$

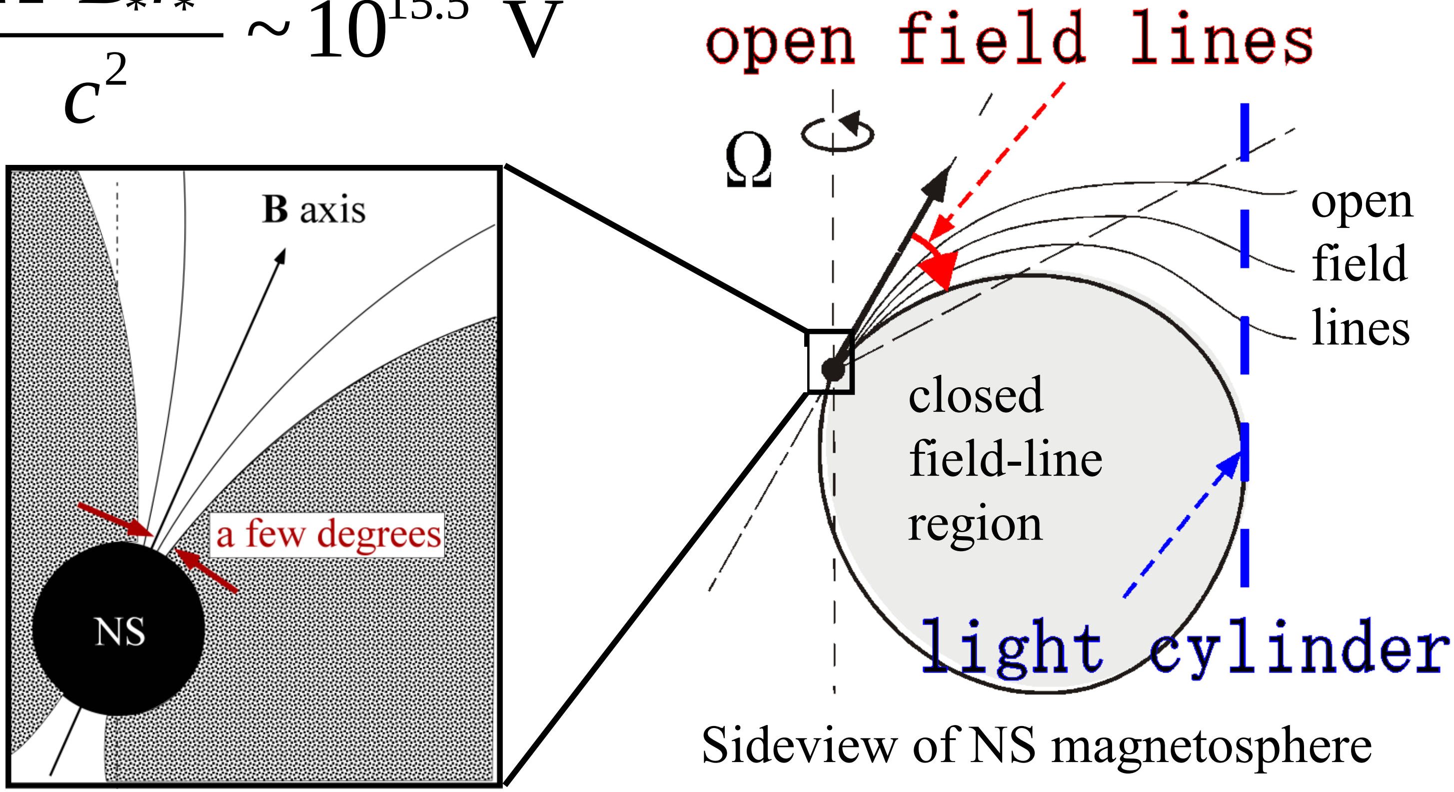

Sideview of NS magnetosphere

§2 Rotating NS Magnetosphere

For typical high-energy pulsars, open zone occupies only a few degrees from ***B*** axis on the PC surface.

Available voltage:

$$\text{EMF} \sim \frac{\Omega^2 B_* r_*^3}{c^2} \sim 10^{15.5}\ \text{V}$$

A fraction (0.1~30%) of this EMF is used for particle acceleration in the magnetosphere.

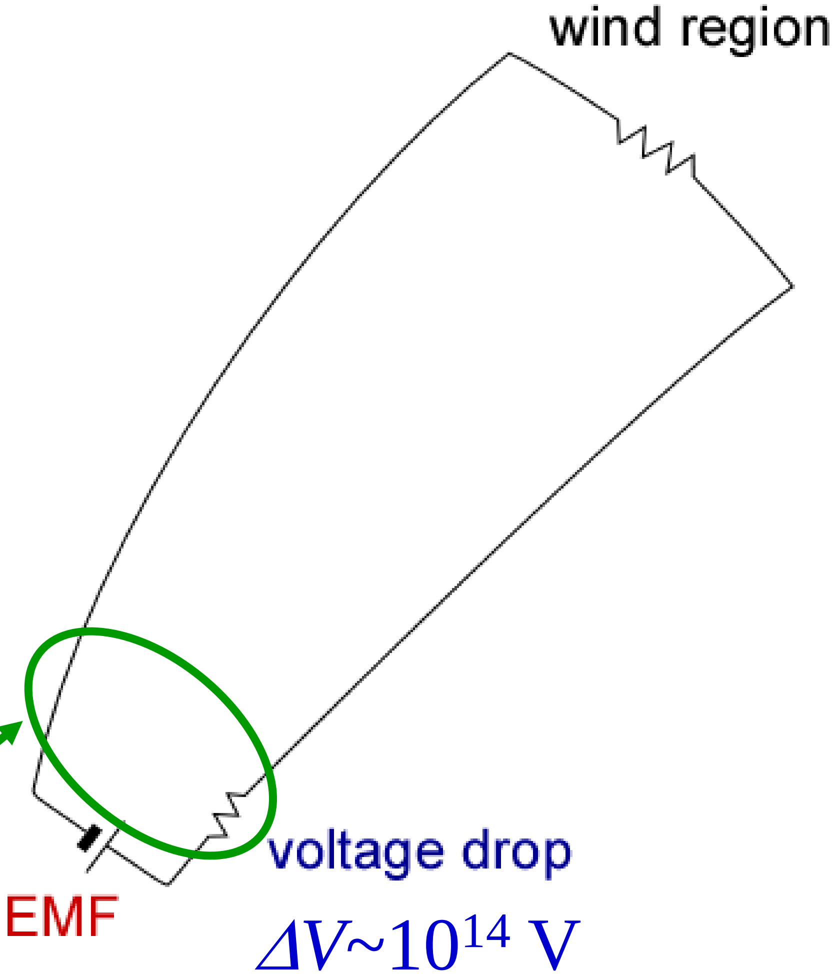

§2 Rotating NS Magnetosphere

In a rotating NS magnetosphere, the Goldreich-Julian charge density is induced for a static observer.
Decoupling **E** into $\mathbf{E}_\perp$ and $\mathbf{E}_\parallel$, we obtain the Maxwell eq.,

$$\nabla\cdot\left(\mathbf{E}_\perp+\mathbf{E}_\parallel\right)=4\pi\rho,$$

where $\rho\equiv e(n_+-n_-)$, and $\mathbf{E}_\perp\equiv -c^{-1}(\mathbf{\Omega}\times\mathbf{r})\times\mathbf{B}$.

Concentrating on the acceleration term, $\nabla\cdot\mathbf{E}_\parallel$, one obtains

$$\nabla\cdot\mathbf{E}_\parallel=4\pi(\rho-\rho_{\mathrm{GJ}}),$$

where

$$\rho_{\mathrm{GJ}}\equiv\frac{1}{4\pi}\nabla\cdot\mathbf{E}_\perp=-\frac{\mathbf{\Omega}\cdot\mathbf{B}}{2\pi c}.$$

§2 Rotating NS Magnetosphere

In a rotating NS magnetosphere, the Goldreich-Julian charge density is induced for a static observer.

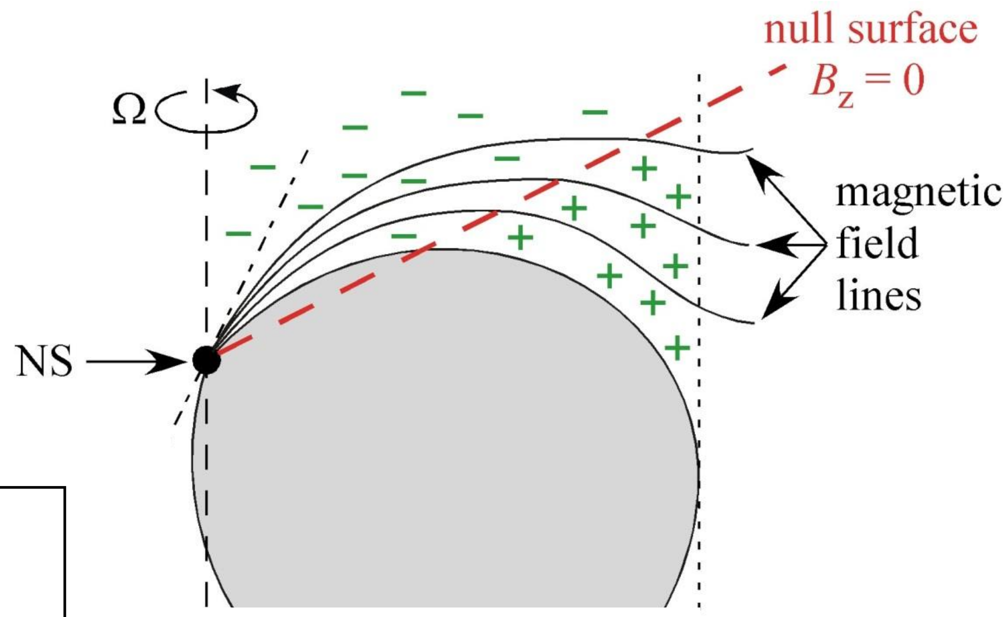

Fig. Goldreich-Julian charge distribution (side view)

Note that ρ_{GJ} changes sign at the null surface.

$$\rho_{\mathrm{GJ}} \equiv \frac{1}{4\pi} \nabla \cdot \mathbf{E}_{\perp} = -\frac{\mathbf{\Omega} \cdot \mathbf{B}}{2\pi c}.$$

(GR expression will be given in chapter 3.)

§2 Rotating NS Magnetosphere

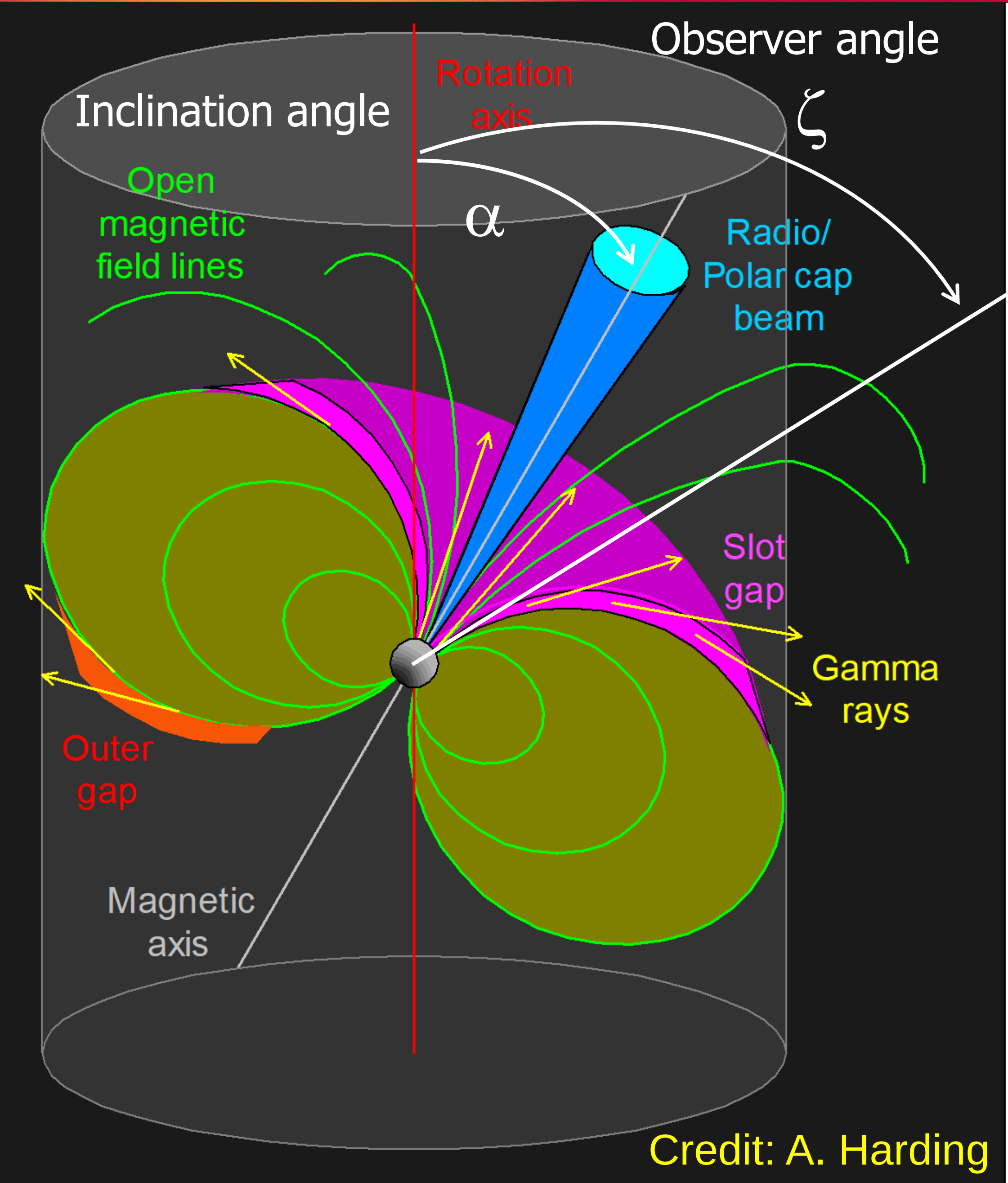

Possible sites of particle acceleration

- Ideal MHD condition holds in most of magnetosphere,
$$E \bullet B = 0.$$
- In some limited regions, deficient charge supply leads to $E \bullet B \neq 0$.
- In charge deficit region, $E_{\|}$ is solved from the Poisson eq.,
$$\nabla \bullet E_{\|} = 4\pi(\rho - \rho_{GJ}).$$

§6 Classic Outer-gap Models

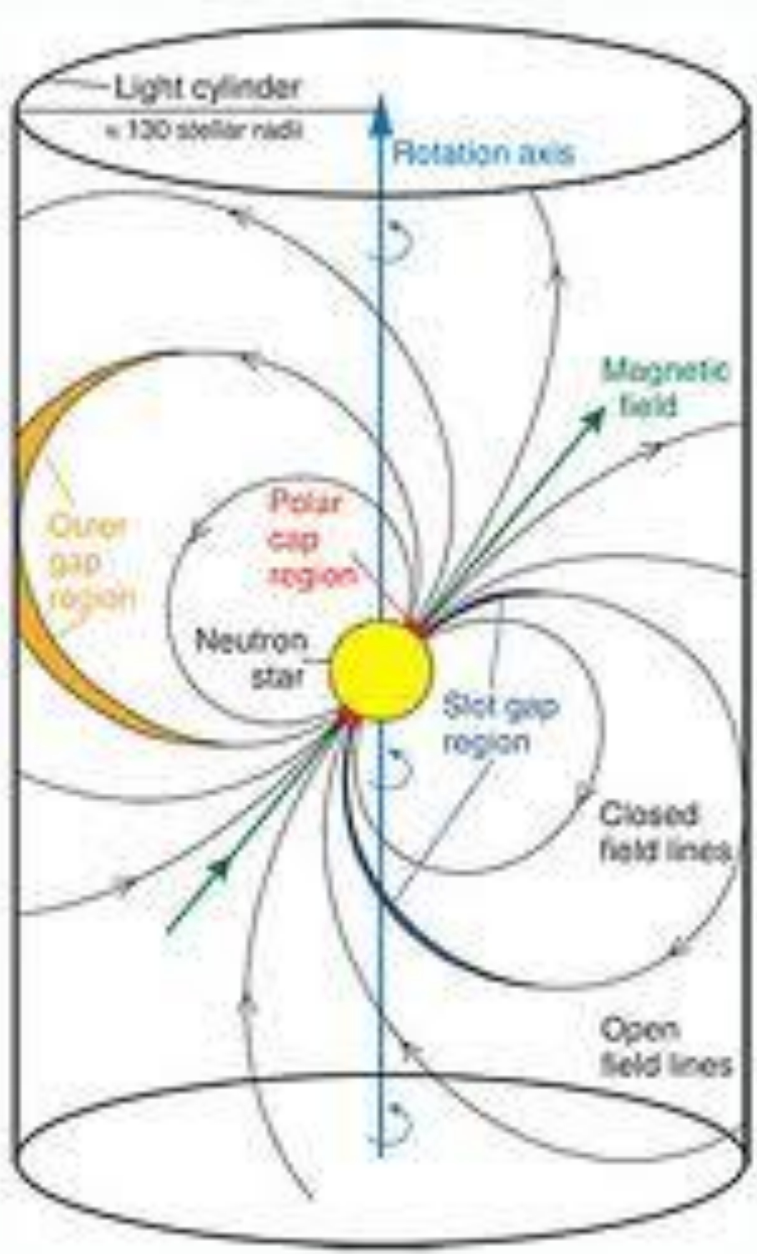

As a possibility of high-altitude emission model, the outer gap model was proposed.

Cheng, Ho, Ruderman (1986, ApJ 300, 500)

So far, there have been found no serious electrodynamical problems in the OG model (unlike SG or PSPC model).

Thus, let us concentrate on the OG model in what follows.

§6 OG Models

Mid 80's, the outer-gap (OG) model was proposed.

(Cheng, Ho, Ruderman ApJ 300, 500, 1986)

Emission altitude > 100 r_{NS} $\longrightarrow$ hollow cone emission

($\Delta\Omega > 1$ ster)

Mid 90s', OG model was further developed by including special relativistic effects. (Romani ApJ 470, 469)

$\longrightarrow$ Explains wide-separated double peaks.

Outer-gap model became promising.

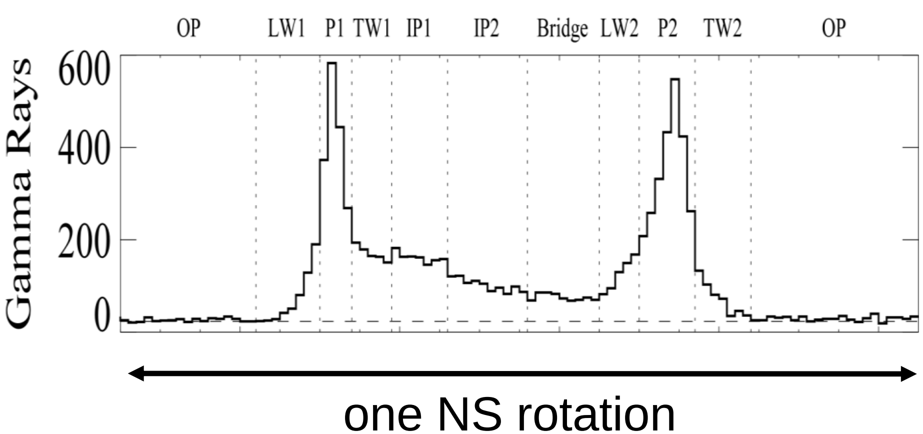

§6 OG Models

OG model reproduces the observed wide-separated HE pulse profiles, which are commonly observed with Fermi/LAT.

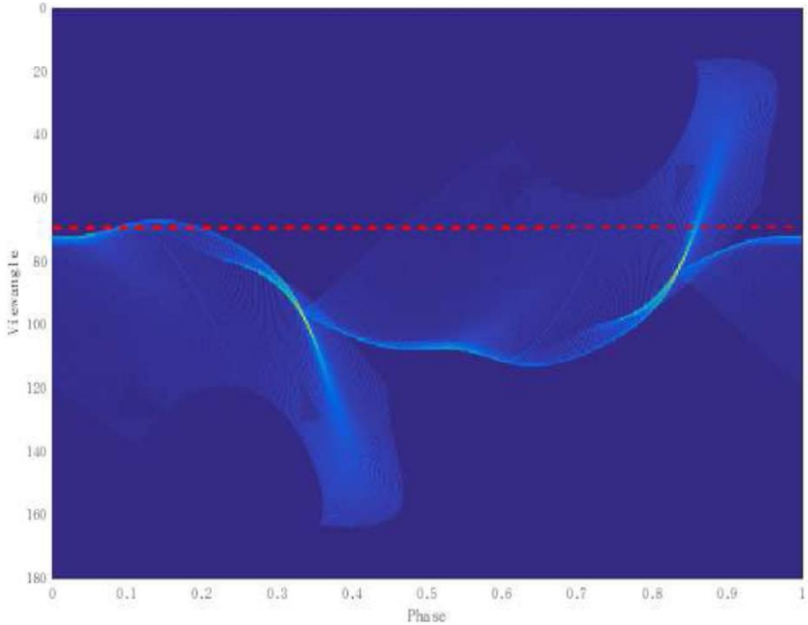

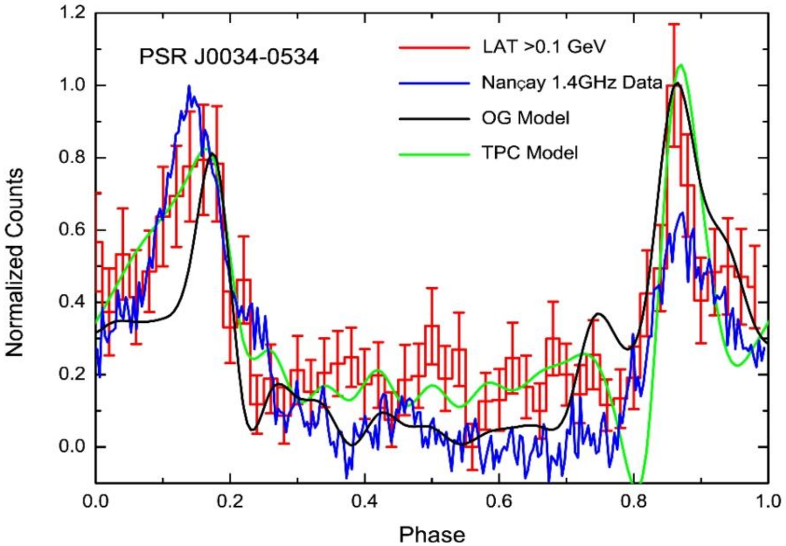

Chang + (2018, MNRAS 475, 2185)

§6 OG Models

OG model predicts the IC emission component whose VHE spectrum is consistent with the IACT observations.

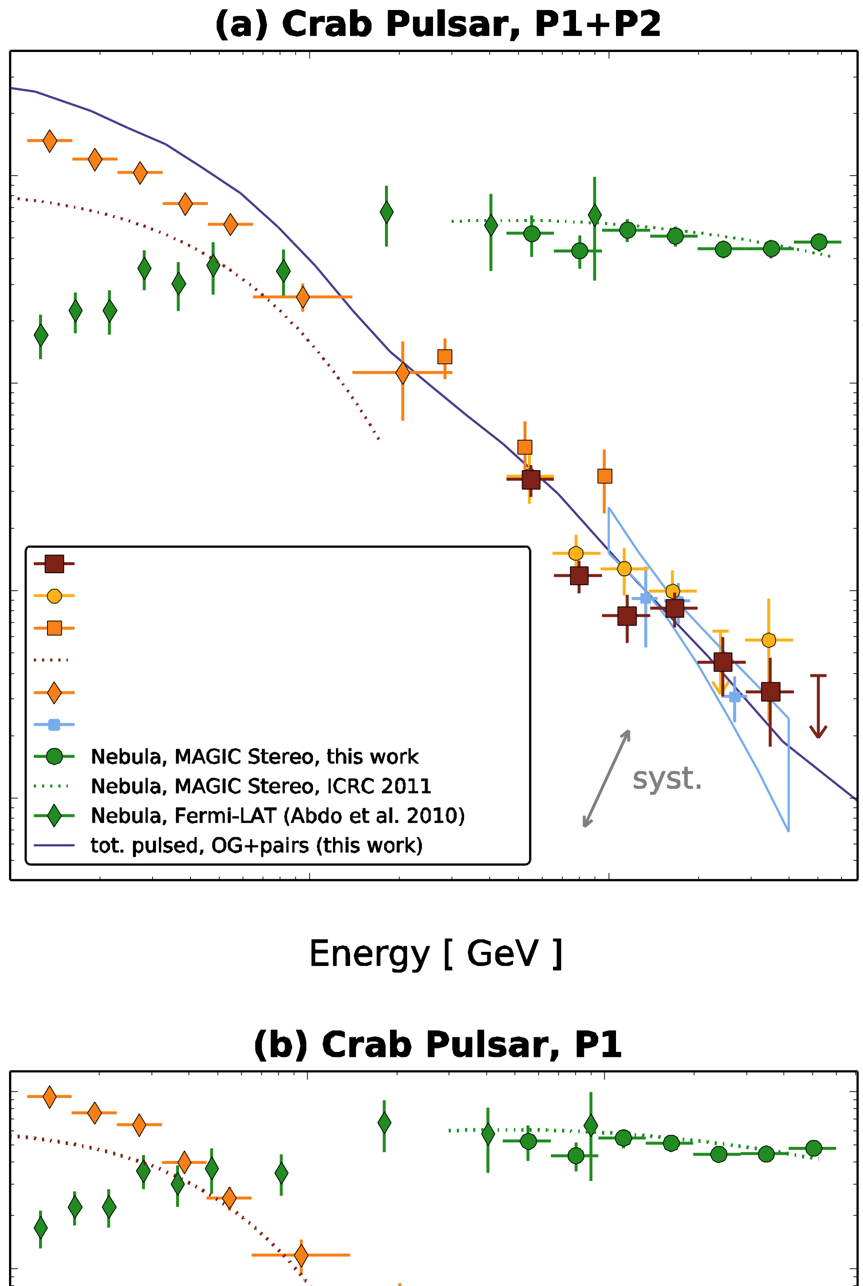

Aleksic + (2012, AA 540, A69)

§6 OG Models

OG model reproduces the observed spin-down vs. γ-ray luminosity relation.

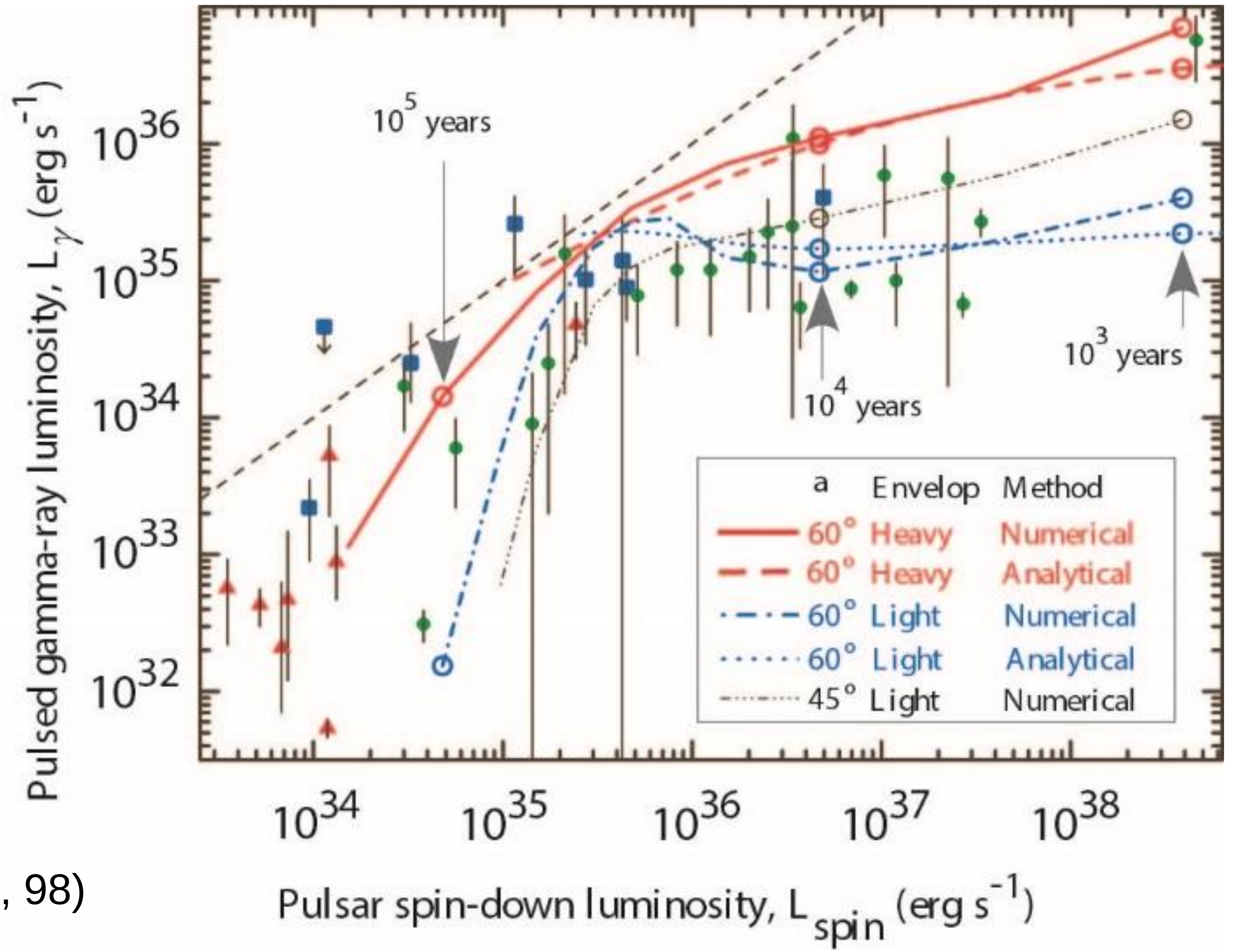

KH (2013, ApJ 766, 98)

§6 OG Models

In short, the pulsar outer-gap model have had success in reproducing various observational properties of HE/VHE pulsars.

In what follows, we apply this successful pulsar emission model to BH magnetospheres and examine the emissions.

END OF CHAPTER 2